PNAS RESEARCH ARTICLE | EARTH, ATMOSPHERIC, AND PLANETARY SCIENCES
ENVIRONMENTAL SCIENCES

Aquatic biomass is a major source to particulate organic matter export in large Arctic rivers

Megan I. Behnke[a,1,2], Suzanne E. Tank[b], James W. McClelland[c], Robert M. Holmes[d], Negar Haghipour[e,f], Timothy I. Eglinton[e], Peter A. Raymond[g], Anya Suslova[d], Alexander V. Zhulidov[h], Tatiana Gurtovaya[h], Nikita Zimov[i], Sergey Zimov[i], Edda A. Mutter[j], Edwin Amos[k], and Robert G. M. Spencer[a]

Edited by Andrea Rinaldo, Ecole Polytechnique Federale de Lausanne, Lausanne, Switzerland; received June 13, 2022; accepted February 4, 2023

Arctic rivers provide an integrated signature of the changing landscape and transmit signals of change to the ocean. Here, we use a decade of particulate organic matter (POM) compositional data to deconvolute multiple allochthonous and autochthonous pan-Arctic and watershed-specific sources. Constraints from carbon-to-nitrogen ratios (C:N), $\delta^{13}C$, and $\Delta^{14}C$ signatures reveal a large, hitherto overlooked contribution from aquatic biomass. Separation in $\Delta^{14}C$ age is enhanced by splitting soil sources into shallow and deep pools (mean ± SD: −228 ± 211 vs. −492 ± 173‰) rather than traditional active layer and permafrost pools (−300 ± 236 vs. −441 ± 215‰) that do not represent permafrost-free Arctic regions. We estimate that 39 to 60% (5 to 95% credible interval) of the annual pan-Arctic POM flux (averaging 4,391 Gg/y particulate organic carbon from 2012 to 2019) comes from aquatic biomass. The remainder is sourced from yedoma, deep soils, shallow soils, petrogenic inputs, and fresh terrestrial production. Climate change-induced warming and increasing CO_2 concentrations may enhance both soil destabilization and Arctic river aquatic biomass production, increasing fluxes of POM to the ocean. Younger, autochthonous, and older soil-derived POM likely have different destinies (preferential microbial uptake and processing vs. significant sediment burial, respectively). A small (~7%) increase in aquatic biomass POM flux with warming would be equivalent to a ~30% increase in deep soil POM flux. There is a clear need to better quantify how the balance of endmember fluxes may shift with different ramifications for different endmembers and how this will impact the Arctic system.

Arctic | rivers | particulate organic matter | endmember | carbon flux

Climate change is warming the Arctic rapidly, modifying permafrost extent and stability with ramifications for carbon cycling globally (1). Disturbed terrestrial carbon can be mobilized in multiple forms including particulate organic matter (POM), which is transported through fluvial networks, modified by estuarine transport, and released to the Arctic Ocean where it can impact oceanic production and chemistry (2, 3). Large Arctic rivers are particularly important POM integrators as they reflect the sum of landscape processes and features in their watersheds and provide a comprehensive picture of the state of the Arctic ecosystem (4, 5).

While there is an ongoing debate about the quantity of permafrost carbon currently being released to rivers (e.g., refs. 6 and 7), fundamental questions concerning how the sources and composition of POM in Arctic rivers will change in response to regional change remain. Permafrost soils are diverse in physical characteristics, chemistry, and hydrology (6, 8, 9) and contain carbon that varies in radiocarbon age from modern ($\Delta^{14}C > 0$; e.g., Heffernan et al. 2020) to ancient, i.e., $\Delta^{14}C < -999‰$ (e.g., ref. 10). However, permafrost is only one possible source of Arctic aged soil organic carbon (SOC). Unfrozen SOC in the pan-Arctic watershed spans a similar age range, i.e., $\Delta^{14}C > 0$ to $< -800‰$ $\Delta^{14}C$ (11, 12), in deep active layers, taliks in permafrost regions, and vast permafrost-free zones that feed north-flowing rivers. Fresh terrestrial production, aquatic biomass, and petrogenic inputs derived from bedrock weathering can also contribute organic matter (OM) spanning a wide range of radiocarbon ages to Arctic rivers, expanding the number of possible sources, and complicating endmember delineation (6, 13–15). Warming temperatures and increasing CO_2 concentrations will lead to greater aquatic primary production (16, 17), modified hydrological processes, and increased potential for soil erosion (9, 18). Collectively, these processes will impact the balance of POM sources entering Arctic rivers, the aquatic carbon cycle, and the ecological functioning of Arctic freshwaters, downstream estuaries, and ocean environments which contribute to the region's ecosystem services to the planet (annual value estimates range from Hong Kong's gross domestic product to the entire global gross domestic product; ref. 19).

Significance

Particulate organic matter (POM) transported in Arctic rivers has previously been viewed as originating primarily from vulnerable northern high-latitude soils. Here, we present results from 8 y of POM sampling from the six largest Arctic rivers, a unique set of mixing models, and endmember data to show that aquatic biomass, a previously overlooked endmember, may contribute 39 to 60% of the average annual 4,391 Gg/y pan-Arctic POM flux. Because of compositional differences, soil-derived POM (like ancient permafrost) has previously appeared to be preferentially preserved in sediments while autochthonous POM (like aquatic biomass) preferentially fuels food webs; this major contribution of in situ riverine production thus suggests a need to reevaluate Arctic riverine POM fate and role in global carbon cycling.

Author contributions: S.E.T., J.W.M., R.M.H., T.I.E., P.A.R., and R.G.M.S. designed research; M.I.B., N.H., A.S., A.V.Z., T.G., N.Z., S.Z., E.A.M., and E.A. performed research; T.I.E. contributed new reagents/analytic tools; M.I.B., S.E.T., J.W.M., R.M.H., N.H., and R.G.M.S. analyzed data; and M.I.B., S.E.T., J.W.M., P.A.R., and R.G.M.S. wrote the paper.

The authors declare no competing interest.

This article is a PNAS Direct Submission.

[1]To whom correspondence may be addressed. Email: mibehnke@alaska.edu.

[2]Present address: Alaska Coastal Rainforest Center, University of Alaska Southeast, Juneau, AK 99801.

This article contains supporting information online at https://www.pnas.org/lookup/suppl/doi:10.1073/pnas.2209883120/-/DCSupplemental.

Published March 13, 2023.

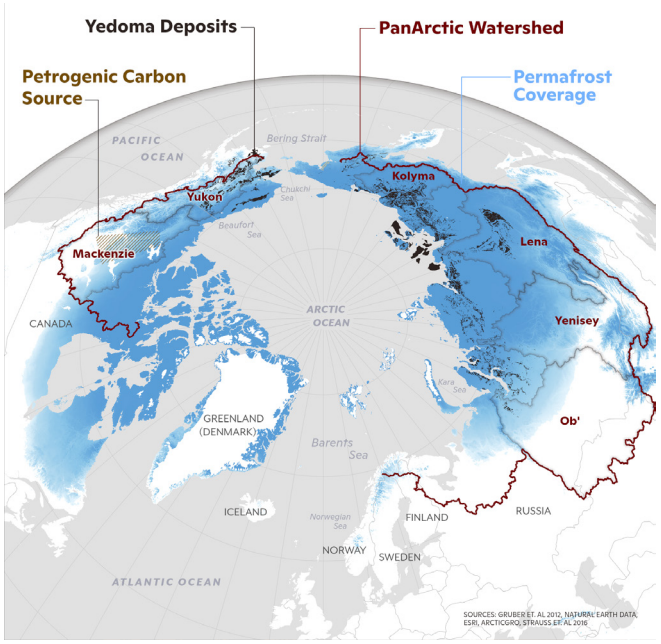

Fig. 1. Map of the six rivers in the Arctic Great Rivers Observatory underlain with the extent and degradation state of permafrost (darker blue indicates more continuous permafrost, lighter blue indicates more discontinuous and sporadic permafrost (8), yedoma deposits (20), and approximate petrogenic carbon source in the Mackenzie (e.g., ref. 21)).

Here, we use 8 y (2012 to 2019) of POM data collected every 2 mo from the six largest Arctic rivers (the Ob', Yenisey, Lena, Kolyma, Yukon, and Mackenzie; Arctic Great Rivers Observatory; www.arcticgreatrivers.org; Fig. 1) to create river-specific, three-tracer mixing models using carbon-to-nitrogen molar ratios (C:N), $\delta^{13}C$, and $\Delta^{14}C$ values to better constrain contributions from different OM sources to POM fluxes. The models use pan-Arctic endmembers gathered from the literature (with sources detailed in Supporting Information) representing autochthonous and allochthonous POM sources as well as river-specific sources and are seasonally explicit (Table 1; refs. 2, 6, 15, and 20). We calculate the flux of each POM source, expressed in terms of particulate organic carbon (POC), and assess how source fluxes partition across rivers and seasons. We explore the notion that aquatic biomass, a POM source previously underappreciated within large Arctic rivers, potentially comprises a major component of the riverine POM pool and contributes substantially to the total POM flux to coastal estuaries. In our analysis, we use an alternative to the traditional division between "active layer" and "permafrost" to capture SOC ages and chemistries encompassing regions that are not underlain by continuous permafrost. We also consider the multifaceted ways that climate change may enable permafrost thaw and shifts in aquatic biomass production to impact the distribution of POM sources and fluxes and how this may affect ecosystem processes such as carbon sequestration and food web productivity.

1. Results

1.1. Sample POC, C:N, $\delta^{13}C$, and $\Delta^{14}C$ Values. Characteristics of surface-suspended POM tended to vary seasonally with discharge, with the lowest POC concentration, highest C:N values, and lowest $\delta^{13}C$-POC values occurring for many rivers in winter (*SI Appendix*, Tables S1 and S2 and Fig. S1) as previously described (5, 6) and notable variation between rivers in the annual cycle of POM characteristics (see *SI Appendix*, Fig. S2 for interannual variation; elucidating interannual trends in POM composition is beyond the scope of this study). The whole POM dataset was depleted in $\Delta^{14}C$ (mean ± SD: −429 ± 149‰) and $\delta^{13}C$ (−29.7 ± 2.5‰) and had low C:N values (11.3 ± 3.7), suggesting inputs of aged carbon as well as nitrogen-rich, $\delta^{13}C$-depleted carbon sources. Spring Mackenzie samples had the lowest $\Delta^{14}C$-POC values (−668 ± 93‰) while spring Ob' samples had the highest values (−249 ± 55‰). As noted previously, the Mackenzie POC was significantly more ^{14}C-depleted across all seasons than all other rivers (Fig. 2; refs. 5 and 21).

1.2. Soil Endmember Delineation. When compiling the data that feed into the soil endmember values, variables did not neatly separate by thaw state or depth (Fig. 3 and Dataset S1). The physical state of many datapoints used in this study was not obvious, while datapoints corresponding to confirmed frozen and unfrozen samples both extended from near surface to >5 m. The near-complete overlap in depth and chemistry of unfrozen (i.e., active layer and nonpermafrost) and permafrost samples in the pan-Arctic watershed renders this delineation unhelpful for our broad assessment. Since there was no obvious break point in SOC chemistry with depth and not all studies reported which soil data were from mineral or organic layers (Fig. 3), we chose to divide the entire soil column into shallow (<1 m) and deep (≥1 m) pools of similar size (537 and 515 datapoints, respectively) to provide a simple demarcation for assessing soil endmembers. Although $\Delta^{14}C$ values vary considerably within each category, those of unfrozen and permafrost categories were more similar (mean ± SD: −300 ± 236 vs. −441 ± 215‰) than shallow vs. deep soils (−228 ± 211 vs. −492 ± 173‰). Thus, sorting soils by depth allows better separation of carbon sources by age than does sorting by thermal state.

1.3. Mixing Model Endmember Contributions to POM Stocks within the Rivers. Across all seasons, aquatic biomass accounted for a majority (seasonal medians >50%) of the POM exported

Table 1. Endmember means ± SDs and sample numbers (*n*) used in the three tracer MixSIAR models

Endmember	$\Delta^{14}C$ (‰)	$\delta^{13}C$ (‰)	C:N	*n* ($\Delta^{14}C$)	*n* ($\delta^{13}C$)	*n* (C:N)
Aquatic biomass*	−106.4 ± 163.8	−33.1 ± 4.7	9.5 ± 3.3	78	132	36
Fresh terrestrial production*	97.0 ± 124.8	−27.7 ± 1.3	91.7 ± 51.1	58	40	58
Shallow soil*	−228.3 ± 211.2	−27.8 ± 1.7	21.4 ± 16.9	308	130	184
Deep soil*	−491.6 ± 172.8	−27.7 ± 1.4	24.0 ± 26.4	287	126	137
Yedoma†	−954.6 ± 66.4	−26.8 ± 2.3	8.6 ± 3.0	214	48	135
Petrogenic‡	−1,000.0 ± 0.0	−24.4 ± 2.4	14.3 ± 0.0	5	10	1

*Endmember used in every river model.
†Endmember used only in the Lena, Kolyma, and Yukon models.
‡Endmember used only in the Mackenzie model.
For endmember value sources see *SI Appendix*.

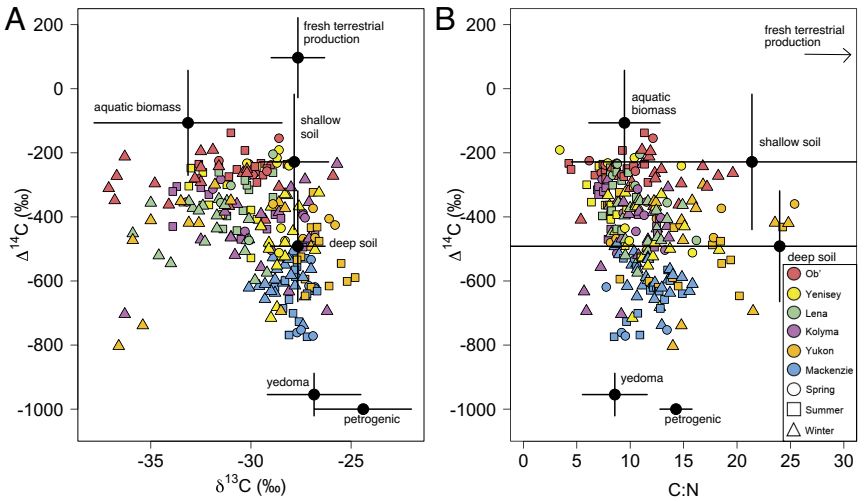

Fig. 2. All samples from all rivers in (*A*) $\Delta^{14}C$ vs. $\delta^{13}C$ space and (*B*) $\Delta^{14}C$ vs. C:N space, with all endmembers and SD ranges for each endmember shown. No single river uses all six endmembers; these are shown for an overview of data only.

by the Ob', Lena, and Kolyma (*SI Appendix*, Table S3). It also contributed substantially to Mackenzie, Yukon, and Yenisey POM (seasonal medians 33 to 44, 8 to 45, and 11 to 53%, respectively; *SI Appendix*, Table S3). Shallow soil provided approximately a third of sampled spring and summer Yukon POM. Deep soil provided 46 to 84% of sampled Yenisey POM. The contribution of fresh terrestrial production was always low (<5%). Yedoma contributed substantially (23 to 43%; *SI Appendix*, Table S3) in all seasons for rivers in which it is present (Yukon, Kolyma, and Lena), while petrogenic inputs made up a majority of the

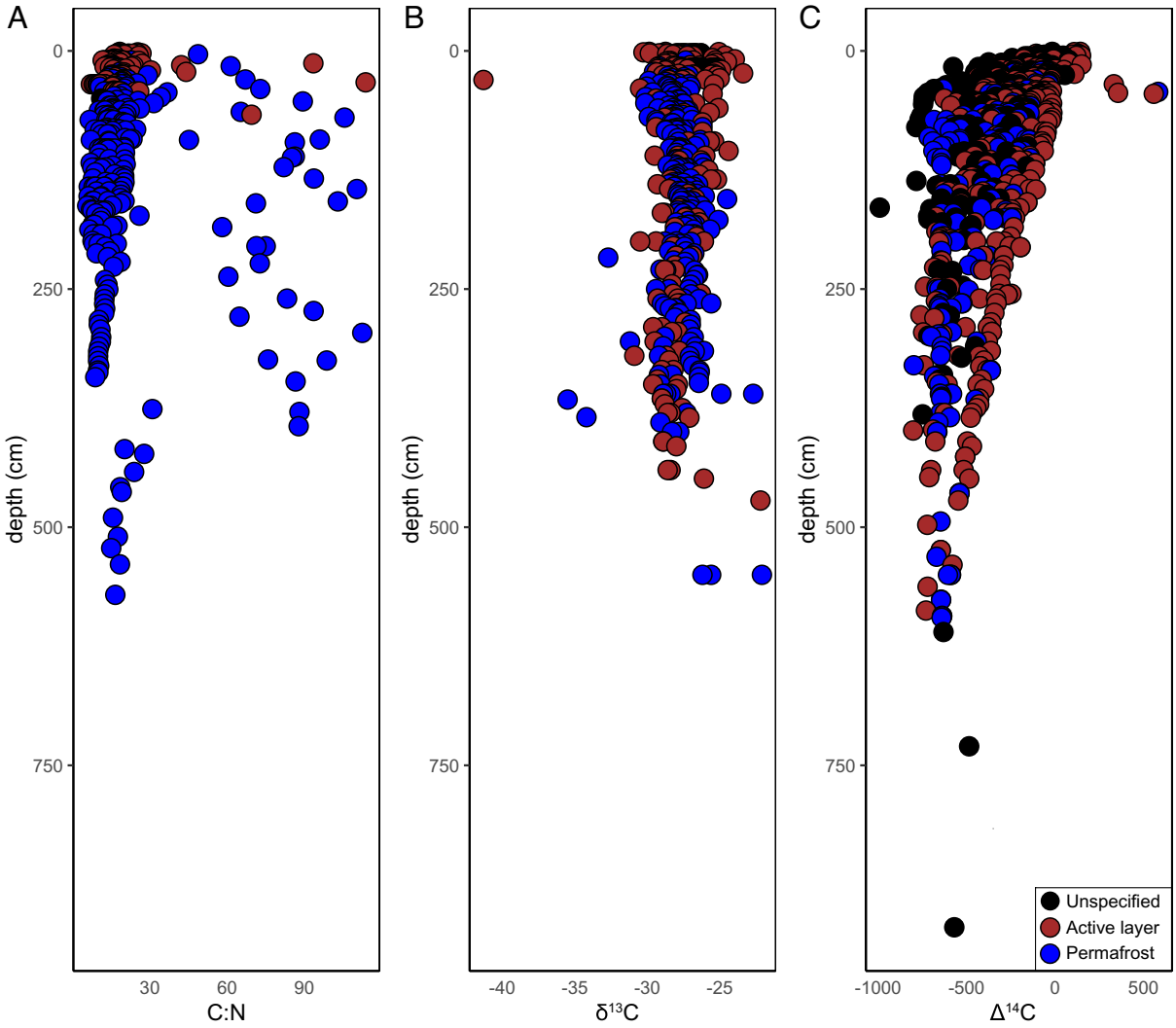

Fig. 3. Samples from literature review used for soil (deep and shallow) endmembers. (*A*) C:N, (*B*) $\delta^{13}C$ values, and (*C*) $\Delta^{14}C$ values for soil organic carbon with depth.

exported Mackenzie POM pool in all seasons (53 to 61%; *SI Appendix*, Table S3).

1.4. POC Fluxes from Each Source. Combining each calculated percent endmember contribution with average POC fluxes for each river and season indicated that aquatic biomass contributed a majority of the pan-Arctic POC flux (median; 5 to 95% credible intervals (CI): 2,219 Gg or 51%; 1,727 to 2,624 Gg or 39 to 60%; Table 2 and *SI Appendix*, Fig. S3 and Tables S3 and S4) and provided the largest annual flux of any endmember in the Ob', Lena, and Kolyma Rivers (*SI Appendix*, Fig. S3). The pan-Arctic contribution of aquatic biomass to POC flux increases from spring to summer to winter (5 to 95% CI of seasonal POC flux 36 to 58%, 43 to 62%, and 44 to 63%, respectively). Yedoma contributed substantially (17; 12 to 21%) to the annual fluvial POC flux across the pan-Arctic despite its presence in only three watersheds, followed by deep soil (12; 5 to 25%). Due to its prevalence and relative importance in the Mackenzie Basin, petrogenic carbon contributed 9% (8 to 10%) to pan-Arctic POC flux, followed by shallow soil (8; 2 to 19%) and fresh terrestrial production (<1; 0 to 3%). All endmembers except yedoma and shallow soil had their largest mean pan-Arctic fluxes during spring, while the largest yedoma and shallow soil fluxes occurred during summer.

Seasonal POC fluxes followed discharge, with the lowest POC fluxes for all rivers during winter low flow (Table 2 and *SI Appendix*, Table S4 and Fig. S3; see also ref. 5). The six rivers export an average of 2,942 ± 150 Gg POC annually over the 2012 to 2019 period [see also the McClelland et al. (5) estimate of 3,055 Gg y^{-1} for 2003 to 2012]. Scaled to the 16.8 × 10^6 km^2 pan-Arctic watershed (Fig. 1), total fluxes result in 2,230 Gg POC (or ~51% annual flux) in spring, 1,918 Gg POC (~44% annual flux) in summer, and 243 Gg POC (~6% annual flux) in fall/winter, or 4,391 Gg POC annually.

Table 2. Mean (SE) fluxes of endmembers for each river averaged across 8 y (except for the Mackenzie, where they are averaged across 6 y) using median (50% CI) endmember contributions

		Ob'	Yenisey	Lena	Kolyma	Yukon	Mackenzie	Sum	Pan-Arctic	% total flux
Total POC flux	Spring	254 ± 11	130 ± 8	446 ± 35	101 ± 25	203 ± 10	480 ± 42	1,494 ± 104	2,230	100
	Summer	286 ± 22	68 ± 3	420 ± 44	55 ± 10	342 ± 20	154 ± 12	1,285 ± 63	1,918	100
	Winter	76 ± 7	29 ± 0	9 ± 1	2 ± 0	30 ± 2	22 ± 2	163 ± 7	243	100
	Annual total	615 ± 33	227 ± 11	875 ± 56	158 ± 34	575 ± 25	656 ± 54	2,942 ± 150	4,391	100
Shallow soil	Spring	8 ± 0	4 ± 0	31 ± 2	5 ± 1	53 ± 2	10 ± 1	108 ± 3	161	7
	Summer	3 ± 0	1 ± 0	8 ± 1	2 ± 0	103 ± 6	2 ± 0	117 ± 6	175	9
	Winter	2 ± 0	1 ± 0	0 ± 0	0 ± 0	2 ± 0	0 ± 0	5 ± 0	7	3
	Annual total	12 ± 1	5 ± 0	40 ± 3	7 ± 2	158 ± 7	11 ± 1	230 ± 9	343	8
Deep soil	Spring	30 ± 1	99 ± 6	22 ± 2	3 ± 1	41 ± 2	10 ± 1	202 ± 7	301	13
	Summer	23 ± 2	31 ± 1	4 ± 0	1 ± 0	51 ± 3	2 ± 0	111 ± 3	166	9
	Winter	15 ± 1	25 ± 0	0 ± 0	0 ± 0	5 ± 0	0 ± 0	45 ± 1	67	28
	Annual total	68 ± 4	154 ± 8	27 ± 2	4 ± 1	96 ± 0	11 ± 1	358 ± 10	534	12
Fresh terrestrial production	Spring	0 ± 0	0 ± 0	4 ± 0	1 ± 0	6 ± 0	0 ± 0	12 ± 0	18	<1
	Summer	0 ± 0	0 ± 0	0 ± 0	0 ± 0	7 ± 0	0 ± 0	7 ± 0	10	<1
	Winter	0 ± 0	0 ± 0	0 ± 0	0 ± 0	1 ± 0	0 ± 0	1 ± 0	1	<1
	Annual total	0 ± 0	0 ± 0	5 ± 0	1 ± 0	14 ± 1	0 ± 0	19 ± 1	28	<1
Aquatic biomass	Spring	213 ± 10	26 ± 2	272 ± 21	54 ± 13	35 ± 2	159 ± 14	718 ± 45	1,072	48
	Summer	254 ± 20	36 ± 2	286 ± 30	33 ± 6	27 ± 2	59 ± 4	680 ± 35	1,015	53
	Winter	58 ± 5	3 ± 0	5 ± 0	1 ± 0	14 ± 1	10 ± 1	89 ± 5	133	55
	Annual total	526 ± 28	65 ± 3	563 ± 37	88 ± 18	75 ± 3	227 ± 19	1,487 ± 66	2,219	51
Yedoma	Spring	–	–	103 ± 8	37 ± 9	63 ± 3	–	203 ± 10	303	14
	Summer	–	–	118 ± 12	19 ± 4	147 ± 9	–	283 ± 19	422	22
	Winter	–	–	3 ± 0	1 ± 0	8 ± 0	–	12 ± 1	18	7
	Annual total	–	–	223 ± 15	57 ± 12	218 ± 10	–	498 ± 25	743	17
Petrogenic	Spring	–	–	–	–	–	293 ± 26	–	–	13
	Summer	–	–	–	–	–	91 ± 7	–	–	5
	Winter	–	–	–	–	–	12 ± 1	–	–	5
	Annual total	–	–	–	–	–	395 ± 33	–	–	9

All fluxes are reported in 1 * 10^9g POC. The pan-Arctic fluxes were estimated by scaling up from the watershed areas of the six rivers to the pan-Arctic drainage basin area (Fig. 1), assuming equivalent areal POC yields and 67% areal coverage. The petrogenic endmember is assumed to only occur in the Mackenzie watershed and is therefore excluded from the upscaling. The percent total flux column shows the percent of the pan-Arctic seasonal or annual flux represented by each source.

2. Discussion

2.1. Pathways for Allochthonous Endmember Contributions to POM. The fluxes and source attributions of POM reported here are determined from width-integrated surface-suspended POM samples and so account for the main water column fluxes but not movement of deeper suspended sediments or river-bottom materials, which are larger, may differ in character and source, and be of higher concentration (14). Therefore, the flux values presented here are conservative. Yedoma and deep soil contributions follow similar seasonal patterns which are indicative of regulation by erosional processes. Contributions of yedoma are prominent where it is present (the Lena, Kolyma, and Yukon watersheds; 25 to 38% annual flux of rivers; *SI Appendix*, Fig. S3), aligning with recently observed yedoma POM riverine mobilization (6). Deep soil contributions are noticeable where yedoma is absent (i.e., the Ob', Yenisey, and Mackenzie). The older yedoma and deep soil pools are vulnerable to release from river bank erosion (5, 18, 22), showing the greatest susceptibility near the end of summer when lateral thaw causes exposed river bank faces to be least protected from erosion (e.g., ref. 23). We found the greatest percent yedoma contributions to the Lena and Kolyma in winter, which may reflect the substantial lag time between upstream thaw and erosion and POM transport time to the river mouths (on the order of several months; ref. 23).

The deep soil endmember shows a similar lag time in the Ob' and Yenisey, with the greatest percent endmember contribution in winter (5 to 95% CI: 10 to 34% and 72 to 91, respectively; *SI Appendix*, Table S3). The same erosional processes that can introduce POM from deeper soil layers to rivers can also carry shallower, younger soils. Shallow soil emerges as a significant source of POM in the Yukon (12 to 43% annual POC flux), where ongoing bank erosion may be facilitated by it possessing the steepest mean watershed slope and the greatest percent coverage of discontinuous permafrost of the six major Arctic rivers (4, 24, 25). The dominance of the petrogenic endmember in the Mackenzie is consistent with previous studies demonstrating significant inputs from the Devonian-age Canol formation of the lower Mackenzie watershed (21, 26). The similarity of our mixing model results for the Mackenzie (petrogenic endmember 55 to 64% annual Mackenzie POC flux) with previous studies (40 to 57% contribution of ancient petrogenic carbon to Mackenzie region sediments; refs. 15 and 21) supports the endmember contribution estimates in the present study. In contrast, other studies have found that POC taken at depth from the water column in the Mackenzie was younger than surface POC and have thus calculated a smaller overall contribution (10 to 30%) to total suspended sediment load from the petrogenic endmember (14, 26). Our surface POM sampling may thus overestimate total petrogenic contribution to the Mackenzie, but our results fit with past conclusions that Mackenzie POM is sourced from a mix of petrogenic and more modern sources, including algae (14).

Fresh terrestrial production was a negligible contributor to POM in all rivers and seasons. Though fresh terrestrial production overlaps with some riverine POM samples in $\delta^{13}C$ space, all POM samples were substantially aged and displayed lower C:N ratios than the fresh terrestrial production endmember (Fig. 2 and *SI Appendix*, Fig. S4). The lack of fresh terrestrial production in our surface POM samples fits with past work demonstrating a "vegetal undercurrent" carrying undegraded plant fragments near the river bottom and suggests that much fresh terrestrial production is likely transported deep in the water column as coarse debris (14). The lower proportion of surface POM assigned to fresh terrestrial production here than to so-termed "recent organic carbon" in Wild et al. (6) is likely caused by our explicit consideration of aquatic biomass.

2.2. Aquatic Biomass as a Critical and Overlooked Arctic River POM Source. Aquatic biomass (water column OM that has grown in situ such as biofilm or invertebrates) accounts for the bulk of the annual pan-Arctic POM flux (5 to 95% CI: 1,727 to 2,624 Gg or 39 to 60%; *SI Appendix*, Table S4 and Fig. S3). The Ob' River Basin's low mean watershed slope and comparative warmth (mean annual air temperature >1 °C) in comparison to the other watersheds likely provide a habitat conducive to autochthonous production (4). The Ob' Basin contains much of the wetlands of the West Siberian Lowlands, which provide extensive low-gradient water bodies that promote aquatic biomass production within the slow-moving water column (27). Further, the Ob' watershed consists of 22.9% cropland (other rivers <7%), contains significant fisheries and aquaculture in its many connected waterbodies, and produces the highest and second highest dissolved phosphorous and dissolved inorganic nitrogen yields of the six rivers (4, 25, 28). The comparatively warm, low-relief, nutrient-rich nature of the river may therefore contribute to its high aquatic biomass signal. Except for winter, the Yukon showed less aquatic biomass contribution than the other rivers (*SI Appendix*, Table S3), consistent with previous studies hypothesizing that its high particulate C:N and low particulate $\delta^{15}N$ values indicate low aquatic production (5, 22). The significant turbidity and rapid flow from the Yukon's multiyear snow field and glacier (24) melt in spring and summer may limit in-stream production and dilute inputs of aquatic biomass from nonglacierized catchments. In general, the contribution of the aquatic biomass endmember to rivers in spring may include dormant or dead aquatic biomass such as biofilms and living or dead material that persisted under winter ice and is flushed out during freshet high flows, as well as actively growing material. In the Eurasian rivers, the contribution of aquatic biomass was highest in summer, which fits with observations in the Kolyma where 45 to 95% of summer POM was recently shown to be autochthonous (29).

The multiple tracers used here allow us to quantify the importance of aquatic biomass, which has previously been overlooked as a contributor to POM in large Arctic rivers (Fig. 2 and *SI Appendix*, Fig. S4). It is well-understood that autochthonous OM may drive ^{13}C-depletion in aquatic systems (30), including in Arctic rivers (5, 31). The low $\delta^{13}C$-POC values in the present study (min: –37.1‰) are consistent with those previously reported for these watersheds (5, 6) and can only be formed with some contribution from autochthonous production (30) as supported by reported relationships between lipid biomarkers, low C:N values, and ^{13}C-POC depletion (13). Since seasonal mean $\delta^{13}C$-dissolved organic carbon (DOC) values are nearly always more enriched in these rivers than are $\delta^{13}C$-POC values, sorption of DOC onto particles is unlikely to contribute to $\delta^{13}C$-POC depletion (32).

Rivers are typically oversaturated with CO_2 produced by terrestrial carbon remineralization (23, 33), which may be recycled into aquatic biomass and contribute to the preaged aquatic biomass endmember radiocarbon signature. Though the tracer used here cannot distinguish between autotrophic or heterotrophic inputs, the CO_2 saturation likely means riverine autotrophy is a recycling of terrestrial carbon, not a sink of atmospheric carbon. However, this does not mean that aquatic biomass can be lumped together with terrestrial sources since its structure and function changes as SOC with an initially higher C:N ratio and more structurally complex tissue recycles through aqueous CO_2 and becomes fixed into the lower C:N, more carbohydrate-rich

biomass of riverine in situ biomass (e.g., refs. 12 and 34). Since C:N ratios and aromatic/aliphatic content can serve as a control of OM biolability (e.g., refs. 34–36), in-stream recycling fundamentally changes the character and thus the fate of POM being exported to Arctic Ocean estuaries. Aquatic biomass therefore needs to be considered separately from allochthonous sources to understand Arctic POM fate.

2.3. Future Refinements of Endmember Values. All endmember values presented here were obtained through an extensive literature review of existing research (*SI Appendix*). This means that the endmember calculations and flux estimates presented here are only as robust as the values obtainable by searching the existing literature. Here, we discuss caveats around endmember sources and improvements that could be made to the endmember delineation in this study and which can be applied to future research.

The negligible flux of POM derived from fresh terrestrial production estimated in this study does not account for the contributions of older, more degraded terrestrial production that makes up shallow and deep SOC. Further, the POM samples in this study were taken from downstream locations, so that upstream contributions of fresh terrestrial production to headwater streams may largely be respired to CO_2 within rivers and partially recycled into aquatic biomass by the time they are accounted for at sampling sites (33, 37).

We chose to differentiate between shallow (<1 m) and deep (≥1 m) soil to derive endmember values rather than the more traditional active layer vs. permafrost demarcation because of the heterogeneity of soil profiles underlying the pan-Arctic drainage area, which spans from the continuous permafrost zone to regions where permafrost is not present, and the lack of separation of soil chemistry based on thermal state (Fig. 3). The term active layer refers to the seasonally thawed, often younger soil present above permafrost (7), but this terminology breaks down in Arctic regions not underlain by continuous permafrost (9). In contrast, shallow and deep soil are accurate descriptions throughout the pan-Arctic. There are significant knowledge gaps in our understanding of SOC with respect to C:N, $\delta^{13}C$, and $\Delta^{14}C$ values in Arctic and sub-Arctic regions. Some studies that provide excellent soil $\Delta^{14}C$ data either do not report C:N and $\delta^{13}C$ (e.g., ref. 11) or show one or the other only as datapoints in figures (e.g., ref. 38), while other studies thoroughly documenting soil C:N and $\delta^{13}C$ do not assess $\Delta^{14}C$ (e.g., ref. 39). This is understandable, given the cost and time constraints of analyses. However, to improve endmember values, spatially representative soil cores would need to be taken around the pan-Arctic and analyzed at multiple depths for C:N, $\delta^{13}C$, and $\Delta^{14}C$, providing a three-dimensional grid of observations. Such a project would be logistically challenging and extremely costly but would eliminate current substantial data gaps.

Similarly, increasing spatially representative sampling of all other endmembers presented here would naturally improve endmember resolution, particularly for aquatic biomass. Some heterotrophic processes such as methanotrophy can transfer carbon from extremely ^{13}C-depleted methane to higher trophic levels and may augment fractionation by aquatic primary production (40), causing a net ^{13}C depletion in the bulk POM pool. Small Arctic rivers can be supersaturated with methane under ice (41), but methanotrophy appears to contribute little to POM and aquatic biomass ^{13}C-depletion compared to fractionation by primary production (42). Therefore, the methanotrophic contribution to riverine CO_2 isotopic composition and autochthonous POM production may often be small. Since our endmember values are based on real aquatic biomass samples, the methanotrophic contribution to aquatic biomass is integrated in the endmember values, though regional variation in methanotrophic contributions where endmember values were not available may be poorly accounted for and an expansion of endmember samples could reveal a larger methanotrophic influence on $\delta^{13}C$ values in some areas.

Although not typically addressed in mixing models, decomposition processes may shift C:N or isotopic composition of OM residue due to selective consumption of certain biochemicals, adding uncertainty to our endmember values. The ^{13}C enrichment or depletion caused by decomposition depends on the ^{13}C content of the most easily degraded compounds and can range from very minor to over ±1‰ (43–45). The effects of decomposition on aquatic biomass isotope ratios and C:N ratios are not well constrained and therefore not included in endmember values here, though the large SD of the aquatic biomass $\delta^{13}C$ endmember helps moderate the difference that decomposition effects might make to the endmember mean. Due to the high relative contribution of aquatic biomass to POM in this study, we examined how much a decomposition signal might impact these endmember flux values by assessing how a ±1‰ shift in the mean $\delta^{13}C$ value of the aquatic biomass endmember changed the endmember contributions in the Ob' (the most aquatic biomass dominated river). Percent endmember contributions for all seasons varied by ≤1%, so we proceeded with our initial literature-derived endmember values for this assessment.

Estimating the isotopic composition of aquatic biomass based on riverine dissolved inorganic carbon (DIC) isotopic values and concentration would provide an alternate, mechanistic method of deriving endmember values. However, few studies provide the seasonally explicit $\delta^{13}C$- or $\Delta^{14}C$-DIC values needed to calculate annual average values for these rivers (e.g., ref. 24), and this method would not provide C:N ratios for aquatic biomass. Future work constraining both seasonal $\delta^{13}C$-and $\Delta^{14}C$-DIC values and improved aquatic biomass endmember sampling in these rivers would greatly help constrain this endmember's contribution to POM flux.

2.4. POM Source Influences POM Fate and Ecosystem Role. The differential fates of autochthonous and allochthonous POM are highlighted in the selective processing of fresh autochthonous OM in water column and sediments and preferential preservation and accumulation of allochthonous POM in inland and marine sediments even when rates of deposition are similar (46–49). In general, POM from autochthonous production is considered more biolabile and of greater energetic value to higher trophic level organisms due to its high nutrient and useful biochemical content compared to soil-derived POM (50, 51). Increasing C:N ratios and ^{13}C-enrichment in various POM pools have been evoked as signs of selective mineralization of lower C:N, ^{13}C-depleted fresh (including autochthonous) POM (2, 26, 52). Further, low C:N, autochthonous POM drives microbial activity in large and small river estuaries (53, 54).

Since mineral association provides long-term OM protection (55), the mineral loads associated with some soil-derived POM fractions may serve as ballast and lead to their preferential deposition (2, 13, 48). Furthermore, deposition and mineral protection within sediments cause POM mineralization rates to decrease substantially especially under anoxic conditions (56–58). Both buoyant, nonmineral-bound organic detritus (2) and POM from marine and estuarine autochthonous production (46, 48, 54) appear to be preferentially transported laterally in estuary or ocean waters or processed rather than being preserved in sediments. We speculate that the same may apply with respect to the aquatic biomass POM flux identified here (Table 2 and *SI Appendix*, Tables S3 and S4), so that POM from aquatic biomass may remain

buoyant and drive secondary production in estuaries or the coastal Arctic Ocean, as has been inferred of Arctic marine autochthonous POM (2, 46, 48, 59).

These fates carry significance for the global carbon cycle. The oldest POM endmembers identified (deep soil, yedoma, and petrogenic carbon; Table 1 and Fig. 2) that together provide a 1,143 to 2,462 Gg annual pan-Arctic POM flux may be preferentially sequestered in sediments (2, 49, 60). In contrast, the aquatic biomass POM endmember should be more readily mineralized and disproportionately fuel food webs (50, 52–54). With its slightly aged signature, it could represent a small leak out of aged high-latitude carbon stocks, but this POM was fixed into its current form relatively recently (within the river system) and likely cycles rapidly (Table 1 and Fig. 2). It is critical to distinguish the contributions of older POM of soil origin (26 to 50%) and more recently fixed aquatic biomass POM (39 to 60%; *SI Appendix*, Table S4), since assuming all or most Arctic river POM has a soil origin ignores potential variation in POM processing rates and their ecological implications for ecosystem services such as fisheries and global climate regulation (19).

2.5. Future Endmember Fluxes in a Warmer World. Riverine POM appears to currently serve as a valuable energy source (3, 53), a vector of carbon sequestration in Arctic Ocean sediments (2, 26, 46, 59), and a source of greenhouse gasses to the atmosphere (56, 57). The terrestrial–aquatic–oceanic system is tightly linked, and terrestrial/aquatic repercussions of warming temperatures and increasing CO_2 levels will influence the future Arctic Ocean (1, 3). Climate change in the Arctic will simultaneously exacerbate permafrost thaw and increase riverine autochthony while at the same time perturbing the hydrologic cycle (1, 17, 18), thus modifying the fluxes of POM endmembers outlined here.

Soil erosion triggered by permafrost thaw may increase the amount of POM sourced from deep and shallow soil and from yedoma and petrogenic sources (7, 18, 22). Given the large flux of allochthonous Arctic river POM to the coast, the fraction of allochthonous POM that may be decomposed either in transit or in sediments still represents a sizable pathway of greenhouse gas emissions (18, 46, 60). However, it appears that much soil POM mobilized by permafrost thaw and erosion may preferentially relocate to storage in aquatic sediments where its decomposition may slow substantially compared to that of buoyant autochthonous POM (2, 26, 56, 58).

Increasing destabilization of soils will also impact autochthonous production and thus the aquatic biomass POM endmember contribution, though the sign of change may depend on the balance between sediment and nutrient mobilization (18). Thaw-induced sediment mobilization can severely decrease stream invertebrate abundance and algal primary production through scouring and shading (61, 62). However, the hypothesized increase in nutrient concentrations in some Arctic flowpaths from thawing permafrost may increase primary productivity and upper trophic level abundances and biomass (18, 63). Warming temperatures and elevated atmospheric CO_2 concentrations will also increase the aquatic biomass endmember directly (16, 17, 64) through increasing primary productivity, greater metabolism potential, and subsequent consumer growth. An increase in aquatic autotrophic production in Arctic rivers may lead to an increase in the bioavailability of exported POM to the estuaries (and after in-transit processing, to the Arctic Ocean) and a concomitant increase in productivity in downstream food webs (49, 50, 54).

A thought experiment about the timing of POM endmember change can help emphasize the importance of differentiating POM sources. Theoretical sediment flux from unregulated Arctic rivers has been estimated to increase 30 to 122% by 2,100 due to ~4.4 °C warming and concomitant increasing discharge (65). Supposing for the purposes of the thought experiment that this increase were to translate into equivalent increases in soil-derived POM and be pan-Arctic in scope, the average annual deep soil endmember flux would increase to 694 to 1,185 Gg (an increase of 160 to 651 Gg annually). This increase in flux would only represent 7 to 29% of the current annual aquatic biomass POM flux estimated in this study. Continuing the thought experiment, benthic algal biomass increased 84 to 405% and phytoplankton biomass increased 32 to 151% under combined elevated CO_2 concentrations and an increase in temperature by 3 °C, ~1.4 °C less warming than assumed above (17, 65). Even the most conservative increase in biomass (17) is greater than the largest estimate of increasing deep soil endmember contributions under warmer conditions. It thus appears likely that a hypothetical 7% increase in the current annual aquatic biomass POM flux will appear far sooner than the equivalent 30% increase in the current annual deep soil endmember flux, particularly since reservoir establishment in Russian rivers appears to actually decrease sediment fluxes (66).

We thus need to pay more attention to quantifying and constraining the timing of POM endmember flux changes, to understand how the balance of future allochthonous and autochthonous POM source contributions could shift the balance of POM sequestration in sediments vs. processing and food web support (52, 60). The 1,249 to 3,290 Gg (5 to 95% CI; 28 to 75% total) annual pan-Arctic flux of POM estimated based on surface samples that are sourced from soils (including older SOC) may increase with increasing thaw and erosion but much of that flux may shift storage locations from the soil column to sediments. Meanwhile, autochthonous riverine production may also increase, fixing a combination of atmospheric and recently respired CO_2. The POM sourced from this aquatic biomass (currently 1,727 to 2,624 Gg, or 39 to 60% annual flux) may fuel Arctic coastal food webs and release carbon from autochthonous production back to the atmosphere.

3. Methods

3.1. Study Location and Sample Collection. Width-integrated samples for POM were collected near river mouths but above tidal influence at Salekhard (Ob'), Dudinka (Yenisey), Zhigansk (Lena), Cherskiy (Kolyma), Tsiigehtchic (Mackenzie), and Pilot Station (Yukon) approximately every 2 mo between summer 2012 and fall 2019 (sampling dates at arcticgreatrivers.org) as part of the Arctic Great Rivers Observatory (Fig. 1) using a previously reported standardized collection method (25). During open water, 1 L of surface water was collected near each riverbank and 2 L were collected from midchannel; samples were combined, kept cold, and filtered the same day. Under-ice samples were obtained from a hole in the ice at mid-channel.

3.2. Sample Analysis. Samples for POC concentrations and stable isotope ratios were filtered through precombusted (450 °C > 5 h) 25-mm Whatman GF/F filters (0.7-μm pore size) with a filter tower and vacuum pump and stored frozen until processing at University of Texas Marine Science Institute. Samples for POC and δ^{13}C-POC analysis were acidified (direct American Chemical Society grade 6% SO_2 minimum H_2SO_3 application for three wetting/drying cycles), while samples for particulate nitrogen (PN) were not. POC, PN, and δ^{13}C-POC samples were run on a Finnigan MAT Delta Plus isotope ratio mass spectrometer interfaced with a Carlo Erba 1500 element analyzer.

Samples for Δ^{14}C-POC were filtered onto 47-mm quartz filters (Whatman QM-A; preashed at 850 °C for 6 h) using a peristaltic pump and inline polycarbonate filter holder. Filters were frozen until acidification using fumigation with HCl and drying at Florida State University. Samples were oxidized to CO_2 using offline dry combustion with CuO, Cu, and Ag at 850 °C in 9-mm quartz tubes.

$\Delta^{14}C$ was measured at the accelerator mass spectrometry facility at ETH-Zurich, where CO_2 was injected into a Mini Carbon Dating System accelerator with a gas-accepting ion source (67).

Differences between rivers for each season and between seasons for each river for carbon isotope values were tested using two-way ANOVA with Tukey's honest significant difference post hoc test using base R (68) and the *agricolae* package (69).

3.3. Mixing Models. Possible contributions of the endmember sources for all POM samples and rivers were calculated using a seasonally explicit, three-tracer mixing model (C:N, $\delta^{13}C$, and $\Delta^{14}C$ of POM) solved using a Markov Chain Monte Carlo method in the MixSIAR package (70) in base R (68), which estimates source contributions accounting for uncertainty in source values, residual, and process errors (71). Endmember values were mined from existing literature determined using previous compilations and Web of Science searches (see *SI Appendix* for complete reference list; Dataset S1; defined in Table 1). A separate three-tracer mixing model was created for each river using endmembers specific to each watershed (Table 1). Fresh terrestrial production, shallow soil, deep soil, and aquatic biomass (comprising algae, biofilm, and invertebrate samples; Dataset S1) were used in the models for all rivers (6, 13, 24), plus a petrogenic endmember for the Mackenzie (21) and a yedoma endmember in the Lena, Kolyma, and Yukon (6, 20). Models were run using endmember means and SDs, with *n* for each endmember set to *n* for whichever variable had the fewest datapoints. MixSIAR models were run without fractionation since the POM source (rather than trophic processes) was analyzed. Each sampling was treated as an individual event. Season was defined as spring (May and June), summer (July–October), and winter (November–April), corresponding to distinct hydrologic phases of high-latitude northern rivers (25), and was included as a "fixed" effect. Models were considered converged when no variables had Gelman–Rubin diagnostics >1.05 (72).

3.4. Flux Calculations. The POC fluxes were generated from yearly discharge data for 2012 to 2019 (2012 to 2017 for the Mackenzie due to missing discharge data) using LoadRunner (73) and the model constituents reported in McClelland et al. (5) and originally generated with discharge data from 2003 to 2011. The model calculates daily flux values using the adjusted maximum likelihood estimation. Fluxes were summed by season, year, and river, with the winter for a year referring to all the winter months in that year (e.g., winter 2012 included January–April 2012 and November–December 2012). POC seasonal fluxes were multiplied by the fractional component each endmember provided (as 50% CI endmember contribution; *SI Appendix*, Table S3) for each season and river to yield endmember fluxes by season and river for each year. Means and SEs for fluxes of each endmember were calculated to obtain average seasonal fluxes (Table 2). Further, each year's endmember contributions from all seasons and rivers were summed and then averaged across year to get the mean total annual contribution of each endmember. The same procedure was used to calculate the 5 and 95% CI endmember contribution fluxes (*SI Appendix*, Table S4).

Data, Materials, and Software Availability. Original particulate organic matter chemistry data have been deposited in NSF Arctic Data Center (DOI: 10.18739/A2D795B9M) (74).

ACKNOWLEDGMENTS. We would like to sincerely thank Bob Hilton and two anonymous reviewers for their insightful comments that greatly improved the manuscript. The NSF supported this work through grants for the Arctic Great Rivers Observatory II (1107774), III (Woodwell Climate Research Center: 1602615; Florida State University: 1603149; University of Texas: 1602680), and IV (WCRC: 1913888; FSU: 1914081; UT: 1914215) as well as an NSF Graduate Research Fellowship to M.I.B. We thank Greg Fiske for creating Fig. 1 and the Laboratory for Ion Beam Physics at ETH Zürich for radiocarbon analyses assistance. Support was also provided by the South Russian Centre for Preparation and Implementation of International Projects (Ob', Lena, and Yenisey), Northeast Science Station (Kolyma), Yukon River Inter Tribal Watershed Council (Yukon), and Les Kutny and the Aurora Research Institute (Mackenzie).

Author affiliations: [a]National High Magnetic Field Laboratory Geochemistry Group, Department of Earth, Ocean, and Atmospheric Science, Florida State University, Tallahassee, FL 32306; [b]Biological Sciences, University of Alberta, Edmonton, AB T6G 2R3, Canada; [c]Marine Science Institute, University of Texas, Port Aransas, TX 78373; [d]Woodwell Climate Research Center, Falmouth, MA 02540; [e]Department of Earth Sciences, Geological Institute, ETH Zurich, Zurich 8092, Switzerland; [f]Laboratory for Ion Beam Physics, ETH Zurich, Zurich 8093, Switzerland; [g]School of Forestry and Environmental Studies, Yale University, New Haven, CT 06520; [h]South Russia Centre for Preparation and Implementation of International Projects, Rostov-on-Don 344090, Russia; [i]Pacific Geographical Institute, Far East Branch, Russian Academy of Sciences, Cherskii 678830, Russia; [j]Yukon River Inter-Tribal Watershed Council, Anchorage, AK 99501; and [k]Western Arctic Research Centre, Inuvik, NT X0E 0T0, Canada

1. M. C. Serreze, R. G. Barry, Processes and impacts of Arctic amplification: A research synthesis. *Global Planet. Change* **77**, 85–96 (2011).
2. J. E. Vonk *et al.*, Preferential burial of permafrost-derived organic carbon in Siberian-Arctic shelf waters. *J. Geophys. Res. Oceans* **119**, 8410–8421 (2014).
3. A. F. Casper, M. Rautio, C. Martineau, W. Vincent, Variation and assimilation of Arctic riverine sestonin the pelagic food web of the Mackenzie River Delta and Beaufort Sea Transition Zone. *Estuaries Coasts* **38**, 1656–1663 (2015).
4. R. M. Amon *et al.*, Dissolved organic matter sources in large Arctic rivers. *Geochim. Cosmochim. Acta* **94**, 217–237 (2012).
5. J. W. McClelland *et al.*, Particulate organic carbon and nitrogen export from major Arctic rivers. *Global Biogeochem. Cycles* **30**, 629–643 (2016).
6. B. Wild *et al.*, Rivers across the Siberian Arctic unearth the patterns of carbon release from thawing permafrost. *Proc. Natl. Acad. Sci. U.S.A.* **116**, 10280–10285 (2019).
7. C. Estop-Aragonés *et al.*, Assessing the potential for mobilization of old soil carbon after permafrost thaw: A synthesis of 14C measurements from the Northern Permafrost Region. *Global Biogeochem. Cycles* e2020GB006672 (2020).
8. S. Gruber, Derivation and analysis of a high-resolution estimate of global permafrost zonation. *The Cryosphere* **6**, 221–233 (2012).
9. M. A. Walvoord, B. L. Kurylyk, Hydrologic impacts of thawing permafrost–A review. *Vadose Zone J.* **15** (2016).
10. L. Schirrmeister *et al.*, Late Quaternary history of the accumulation plain north of the Chekanovsky Ridge (Lena Delta, Russia): A multidisciplinary approach. *Polar Geogr.* **27**, 277–319 (2003).
11. E. D. Schulze, E. Lapshina, I. Filippov, I. Kuhlmann, D. Mollicone, Carbon dynamics in boreal peatlands of the Yenisey region, western Siberia. *Biogeosciences* **12**, 7057–7070 (2015).
12. L. Heffernan, C. Estop-Aragonés, K. H. Knorr, J. Talbot, D. Olefeldt, Long-term impacts of permafrost thaw on carbon storage in peatlands: Deep losses offset by surficial accumulation. *J. Geophys. Res. Biogeosci.* **125**, e2019JG005501 (2020).
13. L. Bröder *et al.*, Particulate organic matter dynamics in a permafrost headwater stream and the Kolyma River mainstem. *J. Geophys. Res.: Biogeosci.* **125**, e2019JG005511 (2020).
14. M. S. Schwab, R. G. Hilton, N. Haghipour, J. J. Baronas, T. I. Eglinton, Vegetal undercurrents-obscured riverine dynamics of plant debris. *J. Geophys. Res. Biogeosci.* **127**, e2021JG006726 (2022).
15. N. J. Drenzek, D. B. Montluçon, M. B. Yunker, R. W. Macdonald, T. I. Eglinton, Constraints on the origin of sedimentary organic carbon in the Beaufort Sea from coupled molecular 13C and 14C measurements. *Mar. Chem.* **103**, 146–162 (2007).
16. I. Ylla, C. Canhoto, A. M. Romaní, Effects of warming on stream biofilm organic matter use capabilities. *Microbial. Ecol.* **68**, 132–145 (2014).
17. N. Fenner, J. Meadham, T. Jones, F. Hayes, C. Freeman, Effects of climate change on peatland reservoirs: A DOC perspective. *Global Biogeochem. Cycles* e2021GB006992 (2021), 10.1029/2021GB006992.
18. J. E. Vonk *et al.*, Reviews and syntheses: Effects of permafrost thaw on Arctic aquatic ecosystems. *Biogeosciences* **12**, 7129–7167 (2015).
19. L. Malinauskaite, D. Cook, B. Davíðsdóttir, H. Ögmundardóttir, J. Roman, Ecosystem services in the Arctic: A thematic review. *Ecosyst. Serv.* **36**, 100898 (2019).
20. J. Strauss *et al.*, "Ice-rich yedoma permafrost: circum-arctic distribution and thickness synthesis" in *Annual Meeting of the "Working Group Permafrost"* (German Society for Polar Research, Hamburg, Germany, 2016).
21. J. E. Vonk *et al.*, Spatial variations in geochemical characteristics of the modern Mackenzie Delta sedimentary system. *Geochim. Cosmochim. Acta* **171**, 100–120 (2015).
22. L. Guo, R. W. Macdonald, Source and transport of terrigenous organic matter in the upper Yukon River: Evidence from isotope (δ13C, Δ14C, and δ15N) composition of dissolved, colloidal, and particulate phases. *Global Biogeochem. Cycles* **20** (2006).
23. I. P. Semiletov *et al.*, Carbon transport by the Lena River from its headwaters to the Arctic Ocean, with emphasis on fluvial input of terrestrial particulate organic carbon vs. carbon transport by coastal erosion. *Biogeosciences* **8**, 2407–2426 (2011).
24. R. G. Striegl, M. M. Dornblaser, G. R. Aiken, K. P. Wickland, P. A. Raymond, Carbon export and cycling by the Yukon, Tanana, and Porcupine rivers, Alaska, 2001–2005. *Water Resour. Res.* **43** (2007).
25. R. M. Holmes *et al.*, Seasonal and annual fluxes of nutrients and organic matter from large rivers to the Arctic Ocean and surrounding seas. *Estuaries and Coasts* **35**, 369–382 (2012).
26. R. G. Hilton *et al.*, Erosion of organic carbon in the Arctic as a geological carbon dioxide sink. *Nature* **524**, 84–87 (2015).
27. A. V. Zhulidov, J. V. Headley, R. D. Robarts, A. M. Nikanorov, A. A. Ischenko, *Atlas of Russian Wetlands: Biogeography and Metal Concentrations* (National Hydrology Research Institute Canada, 1997).
28. M. Korentovich, A. Litvinenko, "Artificial production of Siberian sturgeon fingerlings for restocking the Siberian Rivers of the Ob'-Irtysh Basin: A Synthesis" in *The Siberian Sturgeon (Acipenser baerii, Brandt, 1869)* (Springer, 2018), **vol. 2-Farming**, pp. 181–216.
29. K. Keskitalo *et al.*, Seasonal variability in particulate organic carbon degradation in the Kolyma River, Siberia. *Environ. Res. Lett.* **17**, 034007 (2022).
30. R. Hecky, R. Hesslein, Contributions of benthic algae to lake food webs as revealed by stable isotope analysis. *J. North Am. Benthol. Soc.* **14**, 631–653 (1995).
31. Y. Cai, L. Guo, T. A. Douglas, Temporal variations in organic carbon species and fluxes from the Chena River, Alaska. *Limnol. Oceanogr.* **53**, 1408–1419 (2008).

32. M. Behnke *et al.*, Pan-Arctic riverine dissolved organic matter: Synchronous molecular stability, shifting sources and subsidies. *Global Biogeochem. Cycles* e2020GB006871 (2021), 10.1029/2020GB006871.
33. J. J. Cole, N. F. Caraco, Carbon in catchments: Connecting terrestrial carbon losses with aquatic metabolism. *Marine and Freshwater Res.* **52**, 101–110 (2001).
34. D. Franke, E. J. Bonnell, S. E. Ziegler, Mineralisation of dissolved organic matter by heterotrophic stream biofilm communities in a large boreal catchment. *Freshwater Biol.* **58**, 2007–2026 (2013).
35. J. C. Goldman, D. A. Caron, M. R. Dennett, Regulation of gross growth efficiency and ammonium regeneration in bacteria by substrate C: N ratio. *Limnol. Oceanogr.* **32**, 1239–1252 (1987).
36. P. A. Del Giorgio, J. J. Cole, Bacterial growth efficiency in natural aquatic systems. *Annu. Rev. Ecol. Systemat.* **29**, 503–541 (1998).
37. R. L. Vannote, G. W. Minshall, K. W. Cummins, J. R. Sedell, C. E. Cushing, The river continuum concept. *Can. J. Fish. Aquat. Sci.* **37**, 130–137 (1980).
38. J. Palmtag *et al.*, Storage, landscape distribution, and burial history of soil organic matter in contrasting areas of continuous permafrost. *Arct. Antarct. Alp. Res.* **47**, 71–88 (2015).
39. M. Fuchs *et al.*, Organic carbon and nitrogen stocks along a thermokarst lake sequence in Arctic Alaska. *J. Geophys. Res. Biogeosci.* **124**, 1230–1247 (2019).
40. P. Kankaala *et al.*, Experimental d13C evidence for a contribution of methane to pelagic food webs in lakes. *Limnol. Oceanogr.* **51**, 2821–2827 (2006).
41. C. C. Manning *et al.*, River inflow dominates methane emissions in an Arctic coastal system. *Geophys. Res. Lett.* **47**, e2020GL087669 (2020).
42. J. T. Lennon, A. M. Faiia, X. Feng, K. L. Cottingham, Relative importance of CO2 recycling and CH4 pathways in lake food webs along a dissolved organic carbon gradient. *Limnol. Oceanogr.* **51**, 1602–1613 (2006).
43. R. Benner, M. L. Fogel, E. K. Sprague, R. E. Hodson, Depletion of 13 C in lignin and its implications for stable carbon isotope studies. *Nature* **329**, 708–710 (1987).
44. J. E. Cloern, E. A. Canuel, D. Harris, Stable carbon and nitrogen isotope composition of aquatic and terrestrial plants of the San Francisco Bay estuarine system. *Limnol. Oceanogr.* **47**, 713–729 (2002).
45. N. D. McTigue, P. Bucolo, Z. Liu, K. H. Dunton, Pelagic-benthic coupling, food webs, and organic matter degradation in the C hukchi S ea: Insights from sedimentary pigments and stable carbon isotopes. *Limnol. Oceanogr.* **60**, 429–445 (2015).
46. R. Macdonald *et al.*, A sediment and organic carbon budget for the Canadian Beaufort Shelf. *Mar. Geol.* **144**, 255–273 (1998).
47. M. Fernandes, M.-A. Sicre, The importance of terrestrial organic carbon inputs on Kara Sea shelves as revealed by n-alkanes, OC and δ13C values. *Org. Geochem.* **31**, 363–374 (2000).
48. S. Honjo *et al.*, Biological pump processes in the cryopelagic and hemipelagic Arctic Ocean: Canada Basin and Chukchi Rise. *Prog. Oceanogr.* **85**, 137–170 (2010).
49. F. Guillemette, E. von Wachenfeldt, D. N. Kothawala, D. Bastviken, L. J. Tranvik, Preferential sequestration of terrestrial organic matter in boreal lake sediments. *J. Geophys. Res. Biogeosci.* **122**, 863–874 (2017).
50. F. Guo, M. J. Kainz, F. Sheldon, S. E. Bunn, The importance of high-quality algal food sources in stream food webs–current status and future perspectives. *Freshwater Biol.* **61**, 815–831 (2016).
51. M. T. Brett *et al.*, How important are terrestrial organic carbon inputs for secondary production in freshwater ecosystems? *Freshwater Biol.* **62**, 833–853 (2017).
52. K. Attermeyer *et al.*, Organic carbon processing during transport through boreal inland waters: Particles as important sites. *J. Geophys. Res. Biogeosci.* **123**, 2412–2428 (2018).
53. K. Ziervogel *et al.*, Linking heterotrophic microbial activities with particle characteristics in waters of the Mississippi River Delta in the aftermath of hurricane Isaac. *Front. Marine Sci.* **3**, 8 (2016).
54. P. A. Bukaveckas *et al.*, Composition and settling properties of suspended particulate matter in estuaries of the Chesapeake Bay and Baltic Sea regions. *J. Soils Sediments* **19**, 2580–2593 (2019).
55. J. D. Hemingway *et al.*, Mineral protection regulates long-term global preservation of natural organic carbon. *Nature* **570**, 228–231 (2019).
56. D. C. Richardson, J. D. Newbold, A. K. Aufdenkampe, P. G. Taylor, L. A. Kaplan, Measuring heterotrophic respiration rates of suspended particulate organic carbon from stream ecosystems. *Limnol. Oceanogr. Methods* **11**, 247–261 (2013).
57. M. Repasch *et al.*, Fluvial organic carbon cycling regulated by sediment transit time and mineral protection. *Nat. Geosci.* **14**, 1–7 (2021).
58. S. Peter, A. Isidorova, S. Sobek, Enhanced carbon loss from anoxic lake sediment through diffusion of dissolved organic carbon. *J. Geophys. Res. Biogeosci.* **121**, 1959–1977 (2016).
59. M. S. Schwab *et al.*, Detrital neodymium and (radio) carbon as complementary sedimentary bedfellows? The Western Arctic Ocean as a testbed. *Geochim. Cosmochim. Acta* **315**, 101–126 (2021).
60. S. Shakil, S. Tank, J. Vonk, S. Zolkos, Low biodegradability of particulate organic carbon mobilized from thaw slumps on the Peel Plateau, NT, and possible chemosynthesis and sorption effects. *Biogeosci. Discuss.* 1–25 (2021).
61. B. Levenstein, J. M. Culp, J. Lento, Sediment inputs from retrogressive thaw slumps drive algal biomass accumulation but not decomposition in Arctic streams, NWT. *Freshwater Biol.* **63**, 1300–1315 (2018).
62. K. S. Chin, J. Lento, J. M. Culp, D. Lacelle, S. V. Kokelj, Permafrost thaw and intense thermokarst activity decreases abundance of stream benthic macroinvertebrates. *Global Change Biol.* **22**, 2715–2728 (2016).
63. J. P. Benstead *et al.*, Responses of a beaded Arctic stream to short-term N and P fertilisation. *Freshwater Biol.* **50**, 277–290 (2005).
64. P. Schippers, M. Lürling, M. Scheffer, Increase of atmospheric CO2 promotes phytoplankton productivity. *Ecol. Lett.* **7**, 446–451 (2004).
65. V. Gordeev, Fluvial sediment flux to the Arctic Ocean. *Geomorphology* **80**, 94–104 (2006).
66. S. Zolkos *et al.*, Multidecadal declines in particulate mercury and sediment export from Russian rivers in the pan-Arctic basin. *Proc. Natl. Acad. Sci. U.S.A.* **119**, e2119857119 (2022).
67. M. Ruff *et al.*, On-line radiocarbon measurements of small samples using elemental analyzer and MICADAS gas ion source. *Radiocarbon* **52**, 1645–1656 (2010).
68. R Core Team, *R: A language and environment for statistical computing* (Version 4.2.1, R Foundation for Statistical Computing, Vienna, Austria, 2019).
69. F. de Mendiburu, M. Yaseen, agricolae: Statistical Procedures for Agricultural Research (R package version 1.3-3, 2020).
70. B. Stock, B. Semmens, *MixSIAR GUI user manual v3. 1* (Scripps Institution of Oceanography, UC San Diego, San Diego, CA 2017).
71. B. C. Stock *et al.*, Analyzing mixing systems using a new generation of Bayesian tracer mixing models. *PeerJ* **6**, e5096 (2018).
72. A. Gelman, J. B. Carlin, H. S. Stern, D. B. Rubin, *Bayesian Data Analysis* (Taylor & Francis Milton Park, 2014), **vol. 2**.
73. R. L. Runkel, C. G. Crawford, T. A. Cohn, Load Estimator (LOADEST): A FORTRAN program for estimating constituent loads in streams and rivers (Tech. Rep. No. 4-A5, Colorado Water Science Center, CO, 2004).
74. R. M. Holmes, J. McClelland, S. Tank, R. G. M. Spencer, A. Shiklomanov, Arctic Great Rivers Observatory III Biogeochemistry and Discharge Data, 2017-2019. Arctic Data Center. https://arcticdata.io/catalog/view/doi:10.18739/A2T43J430. Deposited 13 September 2022.